Characterization of CRISPR Mutants Targeting Genes Modulating Pectin Degradation in Ripening Tomato[1][OPEN]

Duoduo Wang,[a] Nurul H. Samsulrizal,[b] Cheng Yan,[c] Natalie S. Allcock,[d] Jim Craigon,[a] Barbara Blanco-Ulate,[e] Isabel Ortega-Salazar,[e] Susan E. Marcus,[f] Hassan Moeiniyan Bagheri,[a] Laura Perez-Fons,[g] Paul D. Fraser,[g] Timothy Foster,[a] Rupert Fray,[a] J. Paul Knox,[f] and Graham B. Seymour[a,2,3]

[a]School of Biosciences, University of Nottingham, Sutton Bonington, Loughborough LE12 5RD, UK
[b]Department of Plant Science, Kulliyyah of Science, International Islamic University Malaysia, 25200 Kuantan, Pahang, Malaysia
[c]Institution of Vegetable Research, Shanxi Academy of Agricultural Sciences, Taiyuan City, China 030031
[d]Electron Microscopy Facility, Centre for Core Biotechnology Services, University of Leicester, Leicester LE1 7RH, UK
[e]Plant Sciences Department, University of California, Davis, California, 95616
[f]Centre for Plant Sciences, Faculty of Biological Sciences, University of Leeds, Leeds LS2 9JT, UK
[g]School of Biological Sciences, Plant Molecular Sciences, University of London, Surrey TW20 0EX, UK

ORCID IDs: 0000-0002-3500-1738 (C.Y.); 0000-0003-0234-1450 (N.S.A.); 0000-0003-4570-5138 (J.C.); 0000-0002-8819-9207 (B.B.); 0000-0002-5495-5684 (S.E.M.); 0000-0001-9461-1316 (H.M.B.); 0000-0002-8567-7074 (L.P.); 0000-0002-5953-8900 (P.D.F.); 0000-0002-9757-9615 (T.F.); 0000-0001-3935-8945 (R.F.); 0000-0002-9231-6891 (J.P.K.); 0000-0001-8365-4947 (G.B.S.).

Tomato (*Solanum lycopersicum*) is a globally important crop with an economic value in the tens of billions of dollars, and a significant supplier of essential vitamins, minerals, and phytochemicals in the human diet. Shelf life is a key quality trait related to alterations in cuticle properties and remodeling of the fruit cell walls. Studies with transgenic tomato plants undertaken over the last 20 years have indicated that a range of pectin-degrading enzymes are involved in cell wall remodeling. These studies usually involved silencing of only a single gene and it has proved difficult to compare the effects of silencing these genes across the different experimental systems. Here we report the generation of CRISPR-based mutants in the ripening-related genes encoding the pectin-degrading enzymes pectate lyase (PL), polygalacturonase 2a (PG2a), and β-galactanase (TBG4). Comparison of the physiochemical properties of the fruits from a range of *PL*, *PG2a*, and *TBG4* CRISPR lines demonstrated that only mutations in *PL* resulted in firmer fruits, although mutations in *PG2a* and *TBG4* influenced fruit color and weight. Pectin localization, distribution, and solubility in the pericarp cells of the CRISPR mutant fruits were investigated using the monoclonal antibody probes LM19 to deesterified homogalacturonan, INRA-RU1 to rhamnogalacturonan I, LM5 to β-1,4-galactan, and LM6 to arabinan epitopes, respectively. The data indicate that PL, PG2a, and TBG4 act on separate cell wall domains and the importance of cellulose microfibril-associated pectin is reflected in its increased occurrence in the different mutant lines.

Many fleshy fruits undergo pronounced softening during the ripening process. Softening is important for flavor development and overall palatability, but also impacts fruit storage, transportability, and shelf life (Klee and Giovannoni, 2011). High quality produce with a long shelf life is essential for the modern supply chain. Current methods for slowing the softening process in tomato (*Solanum lycopersicum*) involve the use of hybrids containing nonripening mutations that in the heterozygous form can enhance postharvest life, but these mutations can also compromise other aspects of ripening including flavor and color development (Kitagawa et al., 2005). A better strategy would be to target the softening process alone.

A substantial amount of work has been undertaken to investigate the genetic and molecular basis of fruit softening. Fruit texture is determined by numerous factors including cell wall structure (Seymour et al., 2013), cellular turgor (Saladié et al., 2007), hydroxyl radical (·OH) attack (Airianah et al., 2016), and cuticle properties (Yeats and Rose, 2013). Remodeling of the cell wall is thought to be a predominant mechanism for inducing softening, involving changes in the complex networks of microfibril and matrix polysaccharides including cellulose, hemicelluloses, pectins, and structural proteins (Keegstra, 2010). The primary cell walls (PCWs) and middle lamellae (ML) of fruits are normally rich in pectin and these pectic polysaccharides have long been known to undergo degradation during the ripening process (Brummell, 2006).

Pectins are the most structurally complex plant cell wall polysaccharides, and three major classes of these polymers have been identified: homogalacturonan (HG), rhamnogalacturonan-I (RG-I), and rhamnogalacturonan-II (RG-II; Atmodjo et al., 2013). Evidence indicates that during ripening these high M_r

polymers are being released from the wall matrix likely through breaking of covalent linkages (Brummell, 2006). The pectic polymers also undergo a loss of neutral sugar side chains (associated with RG-I) and methyl ester groups from HG (Wang et al., 2018). In tomato, strawberry (*Fragaria* × *ananassa*), and many other fruits, these changes are brought about by suites of cell wall-degrading enzymes (see Table 1 in Wang et al., 2018), with varying cocktails of activities in different species.

Over the past 40 years a wide range of enzymes have been investigated to determine which activities are involved in regulating fruit softening. Work on tomato has included the generation of transgenic plants to silence the activity of genes encoding polygalacturonase (PG), pectinesterase, galactanase (TBG), xyloglucan endo-transglycosylase, and expansin (Sheehy et al., 1988; Smith et al., 1988, 2002; Tieman and Handa, 1994; Brummell et al., 1999; Cantu et al., 2008). These experiments have yielded only modest changes in texture of the transgenic fruits. However, in strawberry, a model for nonclimacteric fruits, suppression of either pectate lyase (*PL*) or *PG* resulted in much firmer fruit (Jiménez-Bermúdez et al., 2002; Quesada et al., 2009). More recently, silencing of *PL* in tomato has been shown to inhibit fruit softening (Uluisik et al., 2016). Pectin degradation has therefore been demonstrated to be a major determinate of softening in fleshy fruits.

New insights into the structure of PCWs are providing a way to further characterize the role of pectin degradation in fruit softening. Until recently, pectin was thought to contribute to wall mechanics relatively independently of other cell wall polymers such as cellulose and xyloglucan. The pectic polysaccharides were considered to influence cell wall properties mainly through their ability to form so-called "egg box" structures, in which divalent calcium ions cross-linked chains of de-esterified HG, leading to strengthening of the gel matrix independent of any cellulose-pectin interactions (Carpita and Gibeaut, 1993). In this "tethered network" model, cellulose microfibrils are coated and interlocked by xyloglucan, or other hemicellulose polymers, forming the load-bearing network. However, the validity of this conventional cell wall model has been challenged by a series of recent discoveries. It has been proposed that pectin may directly contribute to the cross linking of cellulose microfibrils in the cell wall, potentially to a greater extent than xyloglucan, the classical cross-linking hemicellulose (Wang and Hong, 2016). Additionally, some subsets of xyloglucan and pectin can be covalently linked together (Thompson and Fry, 2000; Popper and Fry, 2005, 2008; Cornuault et al., 2018) and new structural features of pectic supramolecules have been recognized using atomic force microscopy (Round et al., 2010). They include branches on the main galactosyluronic acid backbone of the pectic polysaccharides. These novel observations may explain why pectin degradation can modulate fruit texture.

For this study, we leveraged available DNA editing technologies (Wang et al., 2014) to generate loss of function mutants in specific cell wall structural enzymes and, therefore, provide an opportunity to revisit their functions in the context of a new understanding of the structure of plant cell walls. We generated mutations in genes encoding the tomato-pectin–degrading enzymes PL, PG2a and TBG4 and analyzed their effects on fruit softening and pectin localization in the ripe fruit pericarp. We report that, in our comparative study, only the silencing of *PL* had any significant impact on tomato softening, and that PL is necessary for: (1) changes in the pectin domains that lead to loss of de-esterified HG from tricellular junctions (TCJs), and (2) degradation of HG and RG-I by PG2a and TBG4. The presence of all three enzyme activities are needed, however, to allow normal ripening-related changes in pericarp cell-to-cell adhesion and solubilization of pectin from association with cellulose microfibrils.

RESULTS

CRISPR/Cas9-Induced Homozygous Lines were Generated to Silence*PL*, *PG2a*, and *TBG4*

Single guide RNAs (sgRNAs) were designed to create individual mutations in the coding sequences of *PL*, *PG2a*, and *TBG4* (Supplemental Table S1). Specific sites were selected to avoid off-target mutagenesis using the tomato genome sequence v2.5 (https://solgenomics.net/). The sgRNAs were expressed under the control of the plant RNA polymerase III AtU6 promoter (Nekrasov et al., 2013). A total of 12, 10, and seven transgenic lines were generated for *PL*, *PG2a*, and *TBG4*, respectively. Two homozygous lines were studied in detail for *PL* and *TBG4*, and three for *PG2a* (Fig. 1). All were fully characterized in the T1

[1]Duoduo Wang was funded by a University of Nottingham Vice-Chancellor's Scholarship and the UK Engineering and Physical Sciences Research Council. Graham Seymour thanks the Biotechnology and Biological Sciences Research Council and Innovate UK for financial support (grant number BB/M025918/1).

[2]Author for contact: graham.seymour@nottingham.ac.uk.

[3]Senior author.

The author responsible for distribution of materials integral to the findings presented in this article in accordance with the policy described in the Instructions for Authors (www.plantphysiol.org) is: Graham Seymour (graham.seymour@nottingham.ac.uk).

G.B.S. and D.W. conceived the original research plans; D.W. performed the majority of the experiments and analyzed the data; D.W. and G.B.S. wrote the manuscript; N.H.S. and C.Y. were involved in generating CRISPR lines; P.D.F. and L.P.-F. undertook the carotenoid analysis and were involved in writing the paper; S.E.M. and H.M.B. performed the cell wall analysis; N.S.A. performed electron microscopy; J.C. provided assistance with statistical analysis; B.B.-U. and I.O.-S. contributed Supplementary Figure S5 and to writing the paper; and T.F., R.F., J.P.K. were involved with writing the paper. All authors were involved in reviewing and editing the manuscript.

[OPEN] Articles can be viewed without a subscription.

www.plantphysiol.org/cgi/doi/10.1104/pp.18.01187

```
WT:      ACGGAAGGGGCGCTAGCGTACACA-T-AGCGGGT
PL5:     ACGGAAGGGGCGCTAGCGTACACATT-AGCGGGT
PL11:    ACGGAAGGGGCGCTAGCGTACACA-TGAGCGGGT

WT:      ATTAAAGTGATTAATGTAC-TTAGCTTTGGA
PG1:     ATTAAAGTGATTAATGTACCTT-----TGGA
PG21:    ATTAAAGTGATTAATGTACTTAGCCTTTGGA
PG34:    ATTAAAGTGATTAATGTAC-TTA-CTTTGGA

WT:      AGAATAGGCCATACAATCTGCCTCCATGGT
TBG4-6:  AGAATAGGCCATACAATCT----CCATGGT
TBG4-8:  AGAATAGGCCATACAATCTGCC-CCATGGT
```

Figure 1. Generation of a range of CRISPR alleles in *PL*, *PG2a*, and *TBG4*. The wild-type sequences and the mutations generated in specific regions of the gene coding sequences are shown. The sgRNA target sequences are in red and insertions in blue. Deletions are indicated by a dotted line. The PAM site is shown in yellow. WT, wild type.

generation. In addition, a transgene free T1 line, which had come through tissue culture, was used as the azygous wild-type control. Analysis indicated that mutations in the CRISPR lines generated PTCs in the mRNAs of the target genes. These resulted in nonsense mutations and truncated, incomplete, and nonfunctional protein products in the mutants (see Supplemental Figs. S1–S3).

PG2a, *PL*, and *TBG4* Gene Expression and Enzyme Activity in the CRISPR Lines

Expression of the *PL*, *PG2a*, and *TBG4* target genes was determined by reverse transcription quantitative PCR (RT-qPCR) using pericarp tissues of red ripe (breaker+7) fruit. Transcripts of all three genes were reduced in the CRISPR mutants compared with azygous lines. A significant ($P < 0.001$) difference in relative gene expression was detected (Supplemental Fig. S4) in the *PG2a* lines. All CRISPR lines would be expected to generate nonfunctional proteins (Supplemental Figs. S1–S3).

PL activity was estimated based on its β-eliminative reaction with cell wall-bound pectin. The basis of the assay was an increase in A_{232} of the clarified reaction mixture due to the release of 4,5-unsaturated products from cell wall preparations as a result of PL activity. This follows the method described by Collmer et al. (1988). Acetone insoluble preparations were used because we found that the enzyme could not be purified away from the cell wall material without complete loss of activity. PL activity in the CRISPR lines was significantly ($P < 0.001$) reduced in comparison with the azygous controls (Fig. 2A). There was residual PL activity in the CRISPR lines and this likely resulted from other PL genes that are weakly expressed during ripening, such as *Solyc05g055510* and *Solyc02g093580* (Supplemental Fig. S5). The reduction of PL activity in the CRISPR knockout lines was consistent with that reported from the RNAi study published recently by Uluisik et al. (2016). PG2a enzyme activity was significantly ($P < 0.001$) reduced in all three independent CRISPR lines when compared with the azygous control at the red ripe (B+7) stage (Fig. 2B). Residual PG activity was detected in these lines and this must arise from the products of other PG-like genes known to be expressed at low levels in ripening tomato (The Tomato Genome Consortium, 2012). Measurement of

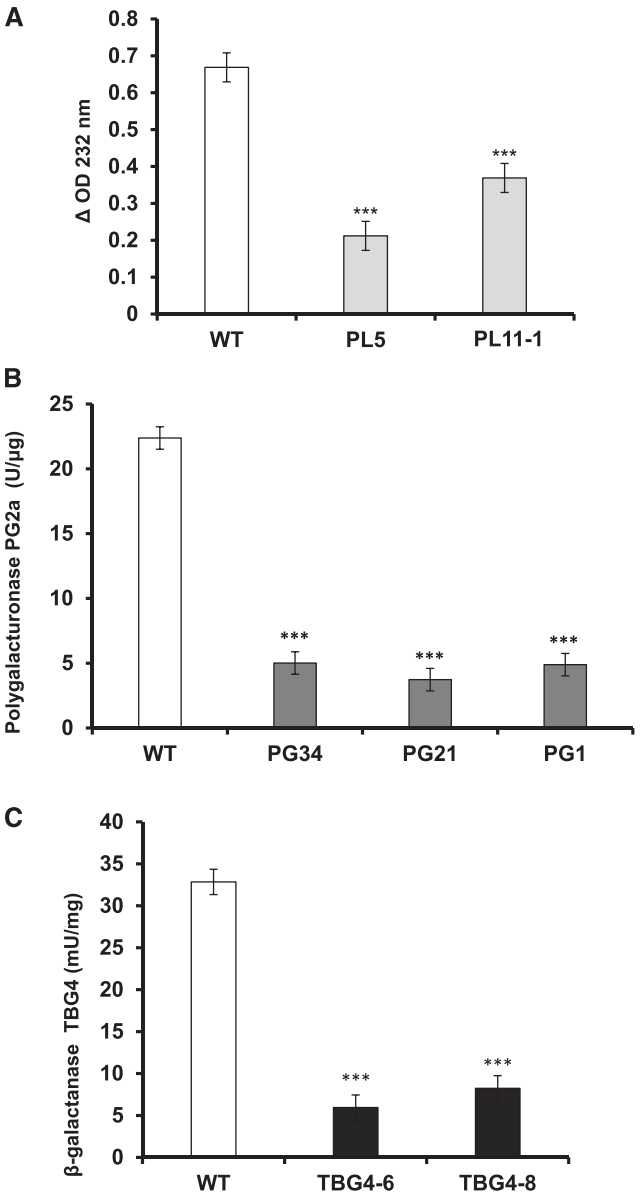

Figure 2. The effect of the CRISPR mutations in the tomato *PL*, *PG2a*, and *TBG4* genes on the activity of the enzymes that they encode. A, PL activity was estimated in the acetone insoluble fraction containing cell wall pectin from two independent CRISPR PL lines. B, PG2a activity was determined by release of reducing groups in three independent CRISPR lines. C, TB-4 activity was determined as release of Gal residues measured in two independent CRISPR lines. Error bars are mean ± SE, $n = 3$. Significant differences between CRISPR lines and the control (wild type) are denoted by (***) ($P < 0.001$) based on a Dunnett's test. WT, wild type.

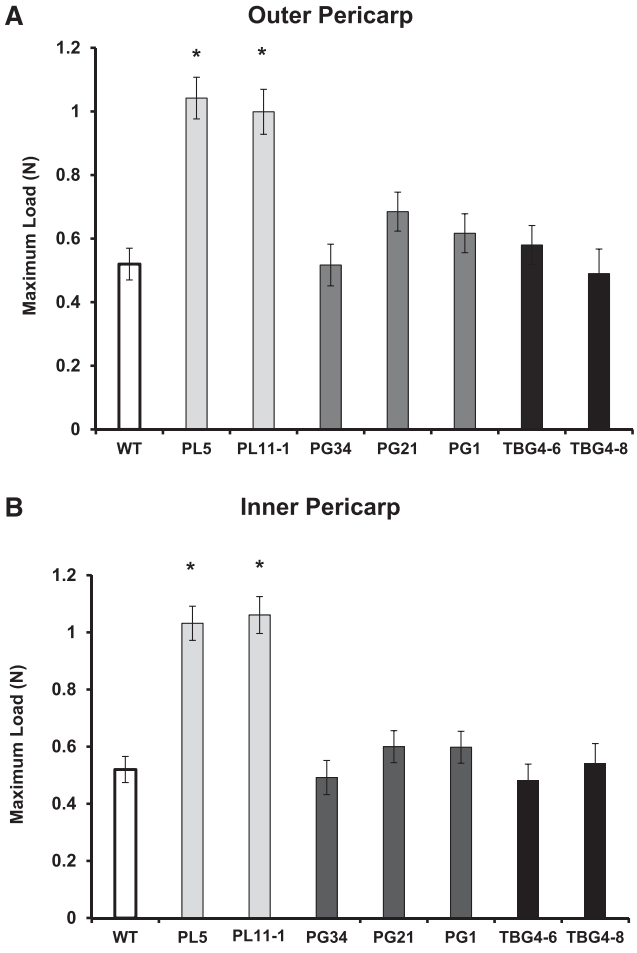

Figure 3. A and B, Effect of CRISPR mutations on fruit pericarp texture. The texture of the pericarp of the different CRISPR lines was compared by measurement of maximum load. There were two *PL*, three *PG2a*, and two independent *TBG4* lines. At least five biological replicates (individual fruits from different plants) from each line were measured for texture line. Significant ($P < 0.05$) differences between a line and the control determined by a Dunnett's test are denoted by (*). Error bars are mean ± SE. WT, wild type.

TBG4 activity was undertaken using a potato β-1,4-galactan-rich substrate. A significant ($P < 0.001$) reduction in enzyme activity was apparent in the *TBG4* CRISPR lines (Fig. 2C). Measurements of total β-galactosidase (Supplemental Fig. S6) did not show a large reduction in the CRISPR lines, but this was expected as most of the β-galactosidase activity in tomato pericarp is associated with other noncell wall-based isoforms (Pressey, 1983).

Effects of CRISPR Mutations on Ripening

Fruits from the *PL* CRISPR lines had significantly ($P < 0.05$) firmer outer and inner pericarp tissues compared to the control, but fruits from the CRISPR edited *PG2a* and *TBG4* lines showed a similar degree of softening to the azygous controls (Fig. 3, A and B). Pericarp color at red ripe B+7 stage was similar in the *PL* and azygous controls. However, a significant ($P < 0.05$) decrease in color index (CI) was detected in both *PG2a* and *TBG4* lines (Fig. 4A). Analysis of pericarp carotenoids indicated significantly ($P < 0.05$) enhanced β-carotene and reduced cis-phytoene in the *TBG4* and *PG2a* lines. There was also a trend toward reduced

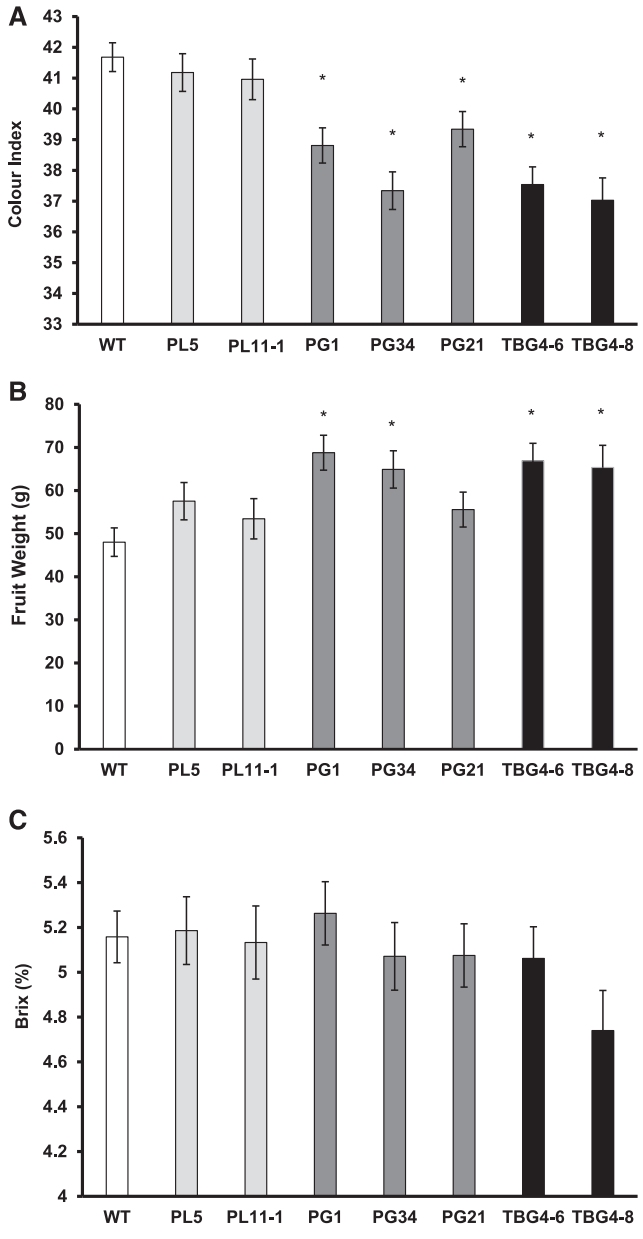

Figure 4. Effect of CRISPR mutations on fruit color, weight, and soluble sugars. Measurements were made of (A) pericarp color, (B) fruit weight, and (C) Brix levels. There were two *PL*, three *PG2a*, and two independent *TBG4* lines. At least five biological replicates (individual fruits from different plants) were measured from each line. Significant ($P < 0.05$) differences between a line and the control (wild type) based on a Dunnett's test are denoted by (*). Error bars are mean ± SE. $n = 5$ or more. WT, wild type.

lycopene levels in these lines, although this was not significant (Supplemental Fig. S7). Such a profile suggests that ripening-related carotenoid formation could have been affected indirectly in these CRISPR mutants. Fruit weight varied among mutant lines. The *TBG4*, *PG1*, and *PG34* CRISPR lines had significantly ($P < 0.05$) higher fruit weights than the azygous control fruit at the same stage of ripeness (Fig. 4B). Measurement of the fresh weight to dry weight ratio (Supplemental Table S2) indicated that the variation among the means was not significant ($P = 0.111$). There were no significant ($P > 0.05$) differences between any of the CRISPR lines and the azygous control in soluble solids content (% Brix) of the fruit at the red ripe B+7 stage (Fig. 4C).

Preliminary assessment of juice viscosity of the CRISPR lines was performed using a RheolabQC rheometer. Juice viscosity was significantly ($P < 0.05$) higher in *PL* and *PG2a* lines compared with the azygous control, with an effect on paste viscosity in one of the *TBG4* lines (Fig. 5). Inhibiting PL and PG activity will permit the structural integrity of pectin polymers to be retained and therefore this would be predicted to have a positive influence on juice viscosity. Investigating the full impact of the CRISPR mutations on tomato processing traits is outside the scope of this investigation and is now part of a further study.

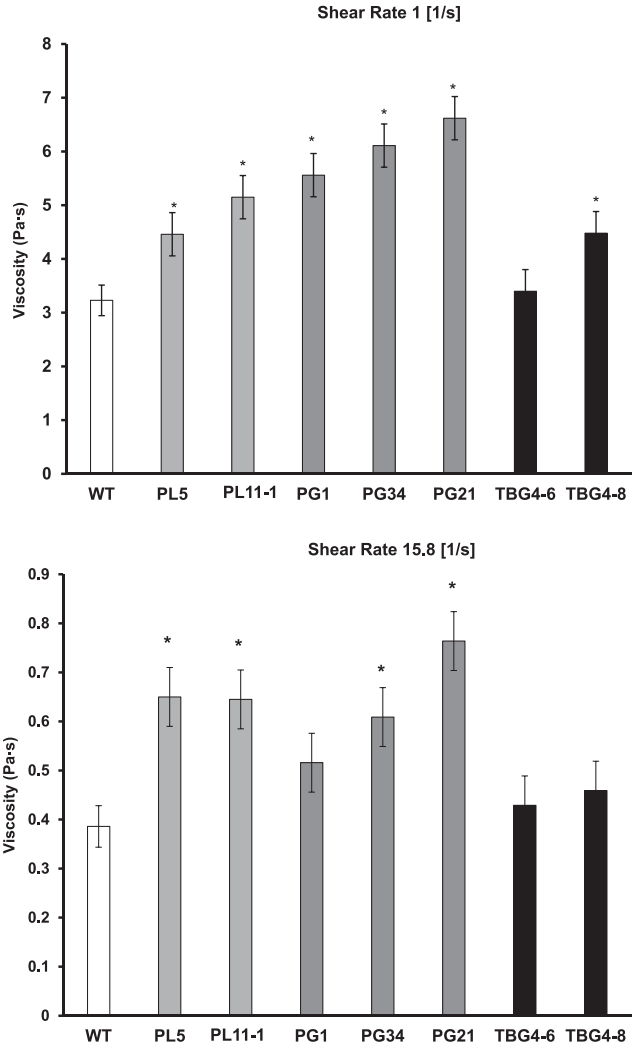

Figure 5. Changes in viscosity of juice generated from CRISPR lines. Stirred viscosity of fruit juice was measured against sheer rates of 1 (top) and 15.8 (bottom) [1/s] using two *PL*, three *PG2*a, and two independent *TBG4* lines. The number of biological replicates was three and error bars are mean ± SE. Samples that were significantly ($P < 0.05$) different from the control determined by a Dunnett's test are denoted by (*). WT, wild type.

Immunocytochemistry of Cell Wall De-Esterified HG and β-1,4-Galactan in CRISPR Mutants

For the immunocytochemistry experiments, a single representative allele from each mutant class was selected and fruit were harvested at the orange ripe B+4 stage. This stage was chosen rather than red ripe B+7 because the activity of each of these cell wall enzymes has previously been shown to be at a maximum post-breaker, but before the fully ripe stage (Della Penna et al., 1987; Smith and Gross, 2000; Uluisik et al., 2016; Yang et al., 2017). Also, preliminary experiments indicated that better fixation and localization of pectin was achieved before fruit becoming fully ripe. All immunocytochemistry experiments were performed using multiple sections taken from embedded pericarp tissue from three biological replicates. The pericarp tissue from each line was fixed, embedded in resin, and thin sections were cut and probed with the monoclonal antibodies LM19 and LM5. LM19 recognizes unesterified HG (Verhertbruggen et al., 2009), LM5 recognizes a linear tetrasaccharide at the nonreducing end of (1-4)-β-D-galactan that occurs as a side chain of RG-I (Jones et al., 1997; Andersen et al., 2016).

Initially, thin sections from each of the lines were labeled with Calcofluor-white, which binds strongly to cellulose (Supplemental Fig. S8). This showed that there were no major differences in cell size or patterning between the tomato lines. Under the transmission electron microscope cell walls of the various lines looked similar (Fig. 6), although electron dense material was more often present in the TCJs of the *PL* and *PG* CRISPR lines. Furthermore, the intercellular spaces in the *TBG4* CRISPR fruits were often larger than in other lines, particularly in the inner regions of the pericarp, indicating some loss of cell-to-cell adhesion at these points (Fig. 6).

Probing the pericarp sections with LM19 indicated a higher epitope signal intensity in the pericarp of *PL*, *PG2a*, and *TBG4* CRISPR lines than that of the azygous control (Fig. 7). In the control, there was some labeling of the cell walls but the epitope was often absent from the cell junctions and ML regions (Fig. 7). Higher levels of labeling with LM19 were apparent in all CRISPR lines. Analysis of the micrographs using the software ImageJ (Supplemental Table S3) indicated that the

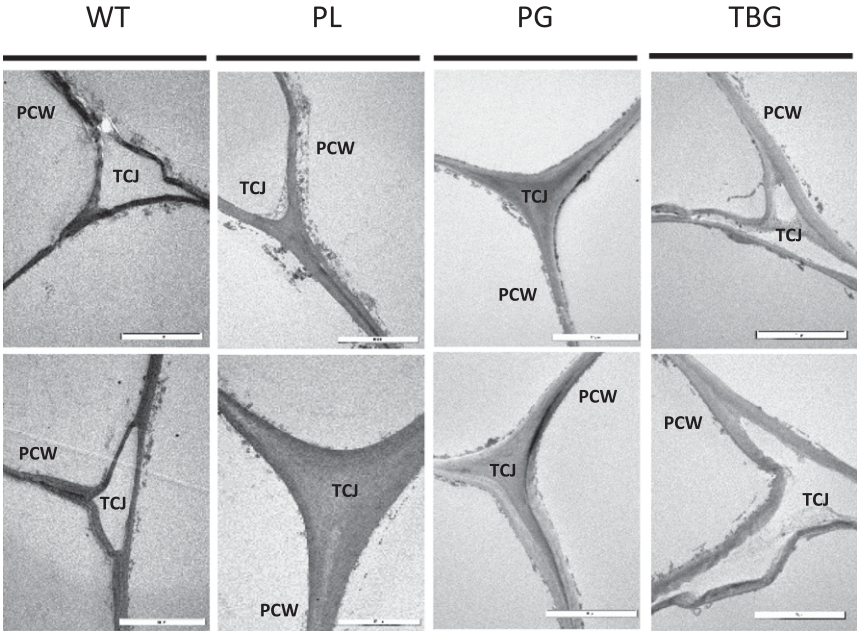

Figure 6. Transmission electron micrographs of cell junctions from the pericarp of the CRISPR lines. Sections cut from three separate fruits from each of wild-type, *PL5*, *PG34*, and *TBG-8* lines were visualized under the transmission electron microscope and two representative micrographs shown for each line. The scale bar on each micrograph represents 10 μm. WT, wild type.

PG2a CRISPR lines had the highest mean intensity of label, whereas azygous controls had the lowest. The intensity of labeling of the sections from the *TBG4* and *PL* CRISPR lines were similar, but higher than the control. There were significant ($P < 0.05$) differences between the labeling intensity in the *PL* and *PG2a* CRISPR lines when compared against the azygous control (Supplemental Table S3).

In sections of the *PL* CRISPR lines, the LM19 epitope was particularly abundant in cell walls at the TCJs (Fig. 7). A distinctive feature of the *PG2a* CRISPR line was the presence of LM19 labeling in the intercellular spaces at some of the TCJs (the point between adherent and separated cell walls). An additional feature of the *PG2a* line was a discontinuous detection of the LM19 epitope in the adhered cell walls. In the *TBG4* CRISPR fruit pericarp, the LM19 epitope occurred evenly in cell walls and was often present in corners of cell wall junctions and partially present in the ML, but absent from the intercellular spaces (Fig. 7).

The monoclonal antibody LM5 was used to detect β-1,4-galactan side chains of RG-I. Low levels of labeling for LM5 were apparent in the azygous control with some labeling in the primary walls, but generally the signal was absent from the ML region. A similar pattern of labeling with LM5 was apparent in the *PG2a* line and the control (Fig. 7). Both the *PL* and *TBG4* CRISPR mutants showed much higher levels of LM5 labeling than the control (Fig. 7, Supplemental Table S3). In the *PL* mutant the outer cell walls of epidermal cells were strongly labeled but the subepidermal cells reacted weakly with LM5, which was in contrast to the *TBG4* CRISPR mutant where subepidermal cells were strongly labeled (Fig. 7). LM5 labeling was evident in the region of the cell wall lining the intercellular spaces especially in the *PL* and *TBG4* lines. In both the *PL* and *TBG4* lines, LM5 binding was generally absent from the intercellular spaces and the TCJs.

Extraction and Characterization of Cell Wall Pectin Fractions Using Pectin Antibody Probes

Cell wall material was prepared from the pericarp of B+7 fruit of representative wild- type, *PL*, *PG2a*, and *TBG4* lines. Preparations of three biological replicates were then extracted sequentially with water, the calcium chelator cyclohexane diamine tetraacetic acid (CDTA), and 4 M KOH and then the residue was treated with cellulase. The clarified extracts were then probed with a range of monoclonal antibodies to determine the levels of specific pectin domains that were solubilized with each extractant (Fig. 8). A substantial additional amount of LM19 positive material was solubilized by water and CDTA in the cell wall preparations from the *TBG4* mutants in comparison to the other genotypes (Fig. 8A). However, significantly ($P < 0.05$) more de-esterified HG was retained in the cellulose residue in the absence of PL, PG2a, or TBG4 in comparison to wild-type controls where all three enzymes were present (Fig. 8A). The LM5 response was significantly ($P < 0.05$) higher in all fractions of the *TBG4* fruit extracts than in the other lines and reduced most in the *PG2a* lines with polysaccharides extracted with water, CDTA, and KOH (Fig. 8B). Galactan-rich pectins were retained with the cellulose residue in the absence of PL and TBG4 activity (Fig. 8B).

As part of the cell wall extraction experiments we tested two additional antibody probes to those used in the immunocytochemistry studies. The INRA-RU1 monoclonal antibody (Ralet et al., 2010) recognizes the RG-I backbone. Significantly ($P < 0.05$) less backbone RG-I epitope was solubilized with water when *PL* and

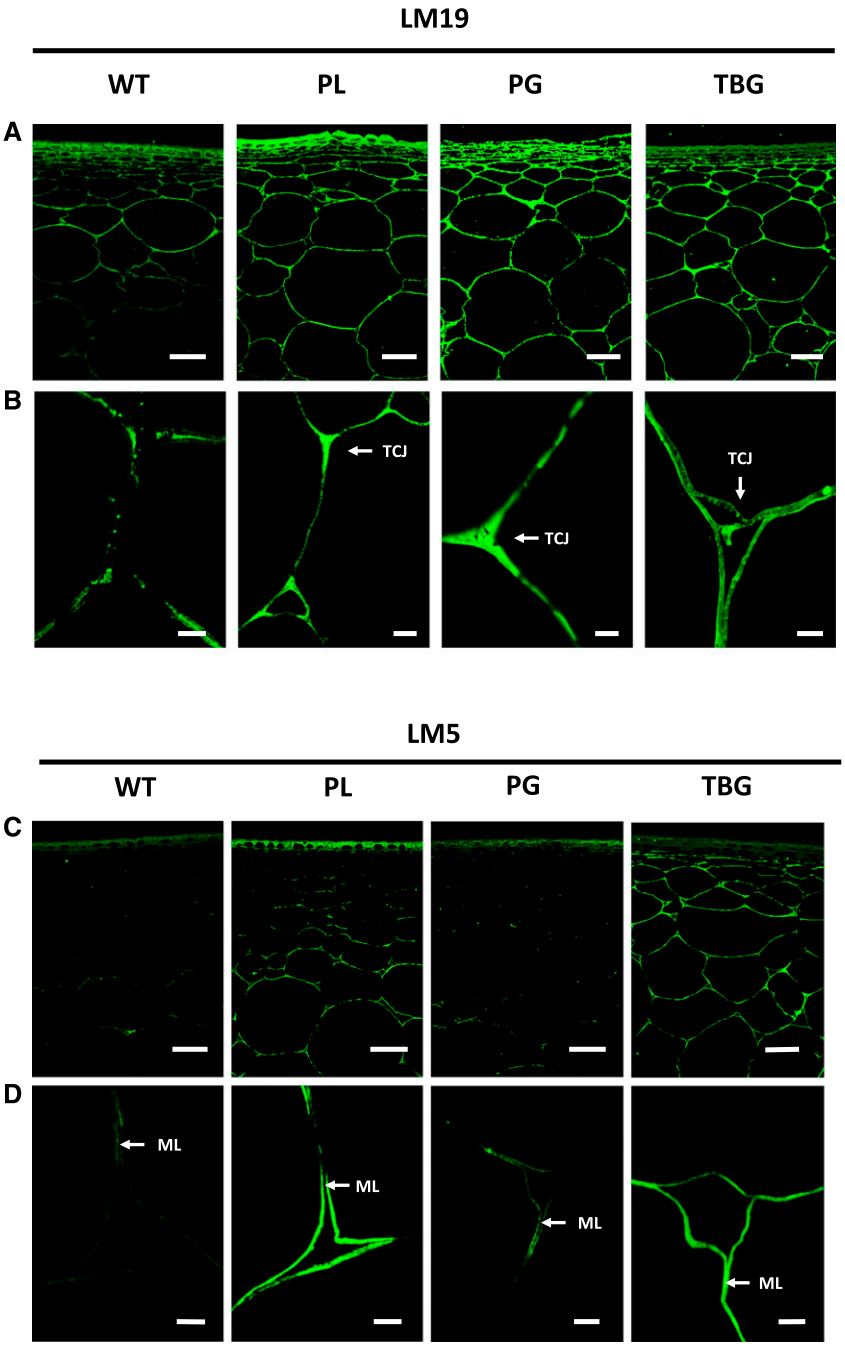

Figure 7. Immunolocalization of deesterified pectin and RG-I in CRISPR lines. Monoclonal antibody probes recognizing deesterified pectin (LM19, top) and pectin-associated β-galactan (LM5, bottom) were used to label tomato pericarp tissue. For each probe, low (A and C) and high (B and D) magnification images are presented. Representative sections of fruits from each of wild-type, *PL5*, *PG34*, and *TBG-8* lines are shown. Scale bar represents 100 μm at low magnification and 10 μm at high magnification. WT, wild type.

PG2a were silenced in comparison to the wild-type lines and the *TBG4* genotype. Conversely, cellulase treatment of residues indicated that more RG-I was associated with cellulose in the absence of PL and PG2a (Fig. 8C). Similarly, for the arabinan epitope of RG-I detected by LM6 (Fig. 8D), lower levels of epitope were solubilized in water and CDTA in the absence of PG2a and higher levels were detected in the cellulase-extracted fraction relative to wild type (Fig. 8D). The use of a postalkali cellulase treatment to release pectic fractions provides an insight into the potential importance of cellulose microfibril-associated pectins.

DISCUSSION

Recent advances in DNA editing have made it possible to precisely manipulate plant genomes. The CRISPR/Cas9 system has been utilized successfully for mutagenesis in a variety of organisms including plants such as Arabidopsis (*Arabidopsis thaliana*; Gao et al., 2016), rice (*Oryza sativa*; Xu et al., 2015; Sun et al., 2016), wheat (*Tricitum aestivum*; Wang et al., 2014), and maize (*Zea mays*; Svitashev et al., 2016). In tomato, genes that have been targeted include *SlAGO7* (Brooks et al., 2014), *RIN* (Ito et al., 2015), *SlPDS* and *SlPIF4*

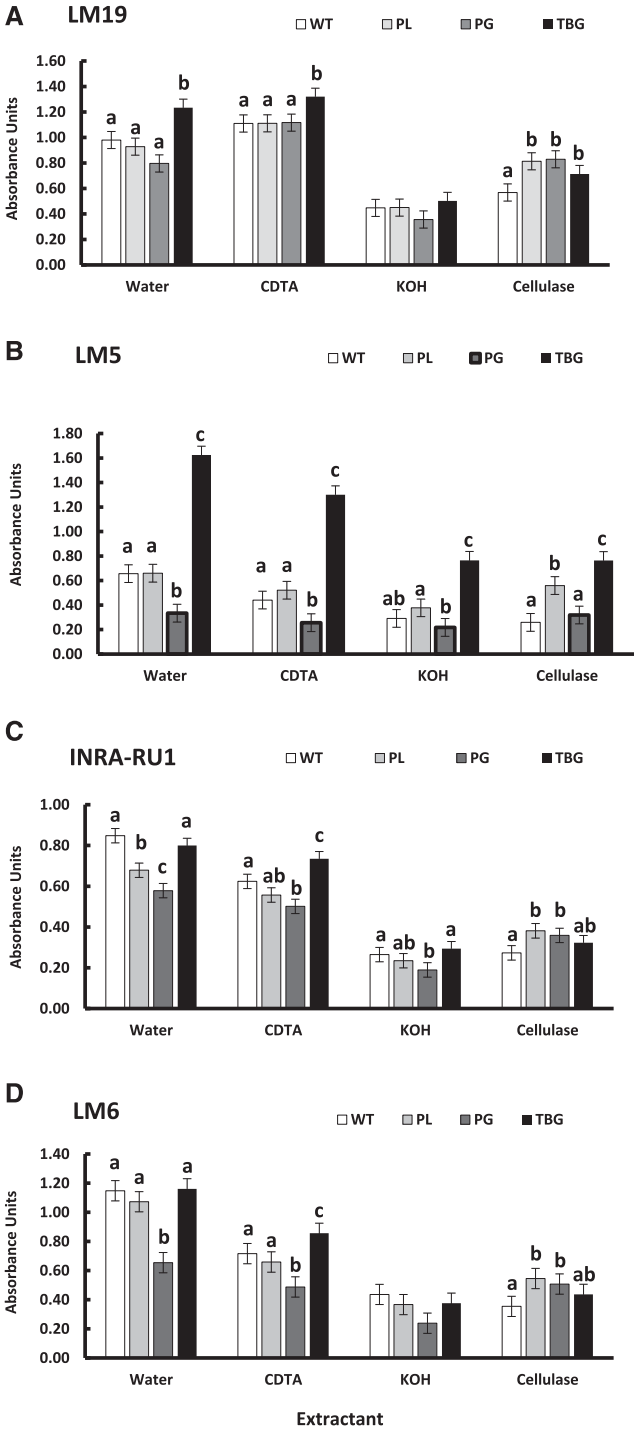

Figure 8. Extraction and characterization of cell wall pectin fractions using pectin antibody probes. Tomato cell wall materials from three biological replicates of breaker+7 fruit pericarp of wild-type, *PL*, *PG2a*, and *TBG4* CRISPR lines were fractionated/sequentially solubilized with water, CDTA, 4 M potassium hydroxide, and by treatment with cellulase. The resulting sequential extracts were serially diluted and analyzed with monoclonal antibodies and data for 6250× dilutions are shown. Antibodies used were (A) LM19 to unesterified HG, (B) LM5 to (1–4)-β-galactan, (C) INRA-RU1- to the RG-I backbone, and (D) LM6 to (1–5)-α-arabinan. Levels of specific pectic polysaccharide epitopes were detected as detailed in the "Materials and Methods." Data were analyzed using a Duncan's multiple range test. Where significant ($P < 0.05$) differences occur between tomato genotypes for the same extractant, these are shown by different letters. WT, wild type.

(*Pan et al., 2016*), and *DELLA* and *ETR1* (Shimatani et al., 2017). Here, we have shown that CRISPR/Cas9 can induce mutations in the genes *PL* (*Solyc03g111690*), *PG2a* (*Solyc10g080210*), and *TBG4* (*Solyc12g008840*), which encode pectin-degrading enzymes. In our study, the CRISPR mutations resulted in a range of transcript abundances with only *PG2a* showing substantial reductions in transcript levels (Supplemental Fig. S4). In eukaryotes, selective mRNAs containing a PTC are targeted for degradation by nonsense-mediated mRNA decay (NMD; Lykke-Andersen and Jensen, 2015) and often associated with decreased mRNA levels compared with their counterparts without PTCs. Both *PG2a* mutant lines have frame-shifts resulting in stop codons being introduced early within the transcript. As such, they are likely to be targets of NMD. The *PG2a* mRNA is one of the most abundant transcripts during normal ripening and this is in part due to its unusually long half-life rather than a particularly high transcription rate (Dellapenna et al., 1987). A switch to rapid turnover as a result of becoming an NMD target will thus have a proportionately strong impact on the *PG2a* mRNA steady-state levels.

All the modified sequences at our target sites were predicted to generate stop codons, and subsequent measures of enzyme activity indicated the CRISPR mutations eliminated the target functions. Interestingly, low ripening-related activities for PL, PG, and TBG were apparent and this residual activity likely reflects the expression in the fruit pericarp of other members of the respective gene families. For example, RT-qPCR data indicates that other *PL* and *PG* genes are being upregulated to some extent to compensate for the mutations in the main ripening-expressed gene family members (Supplemental Fig. S5).

CRISPR Mutations Targeting Pectin Degrading Enzymes and the Impact on Ripening

Before the development of DNA editing technology, antisense RNA and RNAi lines had been generated to silence *PG2a*, *PL*, and *TBG4* (Sheehy et al., 1988; Smith et al., 1988, 2002; Uluisik et al., 2016; Yang et al., 2017). *PG2a* antisense lines showed no effects on fruit texture, although pectin depolymerization was inhibited (Smith et al., 1990). The *TBG4* antisense lines yielded fruit that were reported to be somewhat firmer than those of the control line (Smith et al., 2002). More recently, RNAi lines suppressing *PL* expression resulted in marked effects on tomato fruit texture (Uluisik et al., 2016; Yang et al., 2017).

In this study, using *cv Ailsa Craig* tomato fruits, only the silencing of *PL* resulted in any measurable effect on

fruit softening in contrast to previous reports relating to *TBG4*. The differences between our work and the effects on the *TBG4* antisense fruits reported by Smith et al. (2002) could be due to the genetic background as they performed their experiments in the *cv Rutgers*. The ability of reduced PL activity to delay softening, without impacting other aspects of ripening, was reported in both *cvs Ailsa Craig*, *M82* (Uluisik et al., 2016) and *Micro-Tom* (Yang et al., 2017) indicating a key role for this gene in modulating softening in cultivated tomato. Interestingly, fruits of the *PG2a* and *TBG4* CRISPR lines showed altered color and weight. It has been suggested that pectin oligomers and sugar residues such as Gal, generated by cell wall degradation, could be involved in initiating the ripening process, possibly through induction of ethylene biosynthesis (Gross, 1985; Melotto et al., 1994).

Carotenoid analysis indicated that the changes in pericarp color in the *TBG4* and *PG2a* lines was due to altered β-carotene and lycopene content. A profile of increased β-carotene with a concurrent reduction in lycopene indicates that ripening-related carotenoid formation has been altered, possibly through the modulation of lycopene β-cyclase activity. This enzyme converts lycopene to β-carotene and is normally downregulated at the breaker stage of fruit development (Pecker et al., 1996). In the *PL* CRISPR lines, some pectin degradation may occur due to the activity of the normal *PG2a* and *TBG4* gene products. The delayed color development in the *PG2a* and *TBG4* lines could, therefore, reflect a delay in the onset of ripening. The observed alteration in carotenoid profiles may reflect changes in ethylene perception or response. There was no strong evidence that the differences in fruit weight in the *PG2a* and *TBG4* lines were due to altered water relations in the fruits based on fresh weight:dry weight in the pericarp. Also there was no strong evidence that the fresh weight:dry weight in the PL lines differed from that of the wild type, which was consistent with them both having a similar water content. The difference in fruit weight seen in the *PG2a* and *TBG4* lines merits further investigation.

Previous studies have reported that in tomato, juice produced from transgenic fruit with reduced PG2a activity, modified by antisense technology, was thicker and had a higher viscosity (Schuch et al., 1991; Errington et al., 1998). The properties of tomato juice or paste differ between varieties and are likely to reflect differences in cell wall physiochemical properties between the genotypes (Thankur et al., 1996). Tomato paste is composed of suspended particles including whole cells, broken cells, and cellular fragments in an aqueous serum. In this work, the higher viscosity of the pastes made from the *PL* and *PG2a* CRISPR lines are likely explained by the changes in pectin molecular size resulting from reduced pectin degradation in silencing of these genes (Uluisik et al., 2016). The similarity between *PL* and *PG2a* CRISPR fruits with respect to paste viscosity is consistent with an effect on polyuronide M_rs rather than pectin solubility, which is unaffected in low *PG2a* antisense fruits (Smith et al., 1990), but inhibited in *PL* CRISPR lines (Uluisik et al., 2016). Rheological characterization of juices obtained from transgenic *PL*-silenced strawberry fruits suggested that the increased content of large particles in the juice and the enhanced viscosity were the result of silenced PL activity and improved tissue integrity (Sesmero et al., 2009).

Pectin Localization, Degradation, and Tomato Fruit Softening

The antibody probe LM19 recognizes de-esterified HG. In the *PL* CRISPR mutants, which would be expected to have normal PG2a and TBG4 activity, intense staining of both the ML and TCJ zones was apparent. The *PG2a* CRISPR fruits showed ubiquitous LM19 labeling throughout their cell walls including the ML region, TCJs, and even the intercellular spaces. This was in contrast to the control fruits where some labeling of the primary wall was apparent, but HG appeared absent from other areas. These data support previous findings (Uluisik et al., 2016) that PL is especially important in degrading deesterified HG at TCJs and it has been reported in other plant tissues that the TCJ zones are rich in de-esterified HG (Willats et al., 2001).

The immunolocalization studies indicated that the presence of both normal PG and PL enzymes was necessary to degrade pectin to the extent seen in the wild-type fruits. These data are consistent with previous reports that, in tomato, pectin solubilization requires PL, but PG2a is important for full pectin depolymerization (Smith et al., 1990; Uluisik et al., 2016). Interestingly, in the absence of TBG4 activity in the *TBG4* CRISPR lines, but with *PG2a* and *PL* expression present, the LM19 labels predominantly the PCWs, with some labeling of the ML, TCJs, and no labeling of the intercellular spaces. This indicates that PG2a and PL are necessary and sufficient to degrade deesterified HG in the junction zones. Moreover, the TBG encoded by *TBG4* is needed for full solubilization of de-esterified HG in the ML and PCW, which must be rich in HG and HG linked to RG-I, harboring side chains of β-1,4-galactan.

The LM5 probe, which detects β-1,4-galactan, showed limited labeling in the ML region in the control, *PL*, and *PG2a* CRISPR fruits, which indicates that even in the absence of PL or PG2a, galactans are solubilized from the cell wall and especially the ML. A role for PL in this process was apparent when LM5 labeling of the *PL* CRISPR cell walls was undertaken. There was intense LM5 labeling of the cell walls of both *PL* and *TBG4* mutants. This indicates PL is necessary to facilitate the normal degradation of β-1,4-galactans and as might be expected, the absence of the *TBG4* gene product impacts the solubilization of these polymers and likely RG-I. De-esterified HG has an important role in plant cell wall structure, occurring at points of cell separation such as TCJs and in the ML (Willats et al., 2001), where it mitigates the forces that drive cell separation.

A consistent feature of the parenchyma cells in the *TBG4* CRISPR lines was that the intercellular spaces and junction zones appeared larger and more separated than in the *PL* and *PG2a* CRISPR lines and even the control fruits. A possible explanation for this observation is that in the *TBG4* CRISPR lines, active *PL* and *PG2a* enzymes will have degraded deesterified HG in the cell junctions and ML regions, but RG-I-associated β-1,4-galactans have remained intact. These β-1,4-galactans are thought to reduce flexibility in plant cell walls. For instance, compression tests on pea cotyledons have revealed that galactan-rich cell walls were twice as stiff as those without detectable galactan-rich RG-I (McCartney et al., 2000; Bidhendi and Geitmann, 2016). Therefore, in the absence of HG at TCJs, the presence of galactans in the primary wall may result in elevated levels of separation at the junction zones. This enhanced cell separation may counter-balance the impact of the loss of *TBG4* on fruit firmness. This could explain the variation between the effects of silencing *TBG4* in different tomato backgrounds, as cell wall remodeling changes will likely vary between genotypes depending on the levels of PL, PG2a, and other pectin-degrading enzymes.

To complement the immunocytochemical studies, we investigated the classes of pectin that could be extracted from cell wall material of the different genotypes using a range of solvents. Previous studies indicated that total water-soluble pectin levels are affected by silencing *PL* (Uluisik et al., 2016), but silencing *PG* has limited effects on pectin solubilization (Smith et al., 1990). In this study, we wanted to focus on specific pectin domains to provide more detailed information on the changes in these polysaccharides in mutant and wild-type fruits. The pectin solubilized from the cell wall material was characterized with the same monoclonal antibody probes as for the immunomicroscopy (LM19 and LM5), and two additional probes (INRA-RU1 and LM6), recognizing the RG-I backbone and arabinan epitopes, respectively. LM19 detected elevated levels of water-soluble de-esterified HG in the *TBG4* fruits. Furthermore, these fruits showed enhanced levels of galactan-rich pectin in the water-soluble fractions. These data may reflect the increases in cell separation observed in the *TBG4* fruits, as pectin solubility, cell wall swelling, and presence of intercellular spaces have been linked (Redgwell et al., 1997).

The results of the cell wall analysis were consistent with the immunomicroscopy and demonstrated varying degrees of increased retention (reduced solubility) of HG and galactan-rich pectin in the *PL*, *PG2a*, and *TBG4* lines in comparison to wild-type fruits. There was a significant reduction in the solubility of RG-I and the associated galactan and arabinan epitopes associated with the cellulose residue in all the mutants, and less INRA-RU1 epitope was water-soluble in the *PL* and *PG2a* lines. Published studies on cellulose composites and cellulose microfibrils have indicated that an elevated neutral sugar content of pectin increases the ability of pectin to bind to cellulose. Furthermore, pectin has been observed to accumulate in the spaces of the fibrillar network, as well as adjacent to fibrils. Pectin is likely to coat cellulose microfibrils and affect their level of aggregation (Lin et al., 2016). Cellulose and pectin together have been shown to contribute to the load-bearing capacity of composites during compression. The changes in cellulose microfibril domain structure are likely important in wall toughness and developmental changes including growth (Thomas et al., 2013; Lin et al., 2016), and this may also be the case in fruit ripening.

The importance and role of pectin in cell wall structure is undergoing something of a renaissance. In the generally accepted "tethered network" hypothesis (Carpita and Gibeaut, 1993) the main structural component of the PCW was postulated to be the cellulose microfibrils tethered by hemicellulose molecules. Pectin was thought to form a further independent network with so-called "egg box" structures, in which divalent calcium ions cross-linked chains of demethylesterified HG. Recent studies have indicated, however, that pectin may be much more closely associated with cellulose microfibrils than previously thought. Using solid-state NMR spectroscopy of ^{13}C-labeled Arabidopsis cell walls, it has been demonstrated that pectin-cellulose interactions are extensive and pectin galactan chains may intercalate within, or between, nascent cellulose microfibrils during their synthesis (Dick-Pérez et al., 2011; Wang et al., 2012, 2015; Wang and Hong, 2016). In addition, pectin structure may also involve features that have received little attention in relation to their role in the cell wall such as branching of the main galactosyluronic acid backbone (Round et al., 2010).

The role of HG in cell adhesion and the close association of pectic galactans (RG-I) with cellulose microfibrils is entirely consistent with the observations on the CRISPR mutants made in this study. PL and also the TBG encoded by *TBG4* are necessary for changes in the PCW and ML degradation seen in normal ripening. These changes include the tight control of cell separation, which is enhanced if galactan-rich pectin remains associated with the PCW after degradation of de-esterified HG by PL and PG2a.

The loss of Gal residues associated with the cellulose fraction of cell walls from ripening fruits was observed many years ago (Seymour et al., 1990). This study supports a model where the pectin-degrading enzymes act in a hierarchy to solubilize de-esterified HG and RG-I, leading to tight control of fruit softening and cell separation. We propose that in tomato, PL acts on insoluble high M_r pectic polysaccharides that are associated with cellulose at cell junctions and also on pectin in the ML. The effects of PL involve disaggregation and depolymerization of de-esterified HG (Uluisik et al., 2016). In combination with the action of the TBG, encoded by *TBG4*, HG and RG-I are further solubilized and then HG is depolymerized by PG2a (Smith et al., 1990). Eventually these processes lead to cell separation.

In contrast to tomato, strawberry softening is inhibited to a much greater degree by removal of PG activity (Posé et al., 2015). In this fruit, PG seems to be more active than PL on highly branched pectin in the cell wall. Also, in strawberry, silencing of a cell wall β-galactosidase resulted in firmer fruits (Paniagua et al., 2016). The reason for this variation between species is unclear, but may reflect differences in cell wall composition or the levels of other additional wall-modifying activities that include remodeling of the interactions between pectin and other wall components, such as cellulose, which have often been ignored in previous studies. This may also explain why the effects of silencing of specific genes such as *TBG4* depends on the tomato genetic background. This is illustrated by the observation that in *cv Rutgers TBG4* down-regulation impacts fruit softening (Smith et al., 2002), while mutations in this gene did not influence texture in *cv Ailsa Craig* in this study. These results emphasize the complexity of cell wall remodeling and its effects on plant phenotypes.

MATERIALS AND METHODS

Construction of Cas9/sgRNA-Expressing Vectors

The sites used for targeted mutagenesis were designed according to Shan et al. (2014) using the CRISPR-PLANT tools and the tomato genome sequence database (www.solgenomics.net; Tomato Genome Consortium, 2012) and are listed in Supplemental Table S1. The construction of the AtU6p::sgRNA vector and the Cas9/sgRNA-expressing vectors were based on Golden Gate cloning technology. The sgRNAs were amplified using primers described in Supplemental Table S4 using the plasmid pICH86966:: AtU6p::sgRNA PDS construct (Addgene plasmid 46966) as a template. sgRNAs placed under the Arabidopsis (*Arabidopsis thaliana*) U6 promoter were cut-ligated with the pICSL01009::AtU6p level 0 (Addgene #46968) module into pICH47751 level 1 vector (Addgene #48002) using the Golden Gate cloning method (Weber et al., 2011). The sgRNA-Cas9 plant expression vectors were constructed by performing cut-ligation reaction with level-1 modules pICH47732::NOSp::NPTII (Addgene #51144), pICH47742::35S::Cas9 (Addgene #49771), pICH47751:: AtU6p::sgRNAs, and the linker pICH41766 (Addgene #48018) into the level-2 Golden Gate vector pAGM4723 (Addgene #48015) using *Bbs*I as described by Weber et al. (2011). The complete nptII-Cas9-sgRNA expression cassette was sequenced to verify that the clones had the correct transgene.

Plant Materials, Growth Conditions, and Generation of Transgenic Plants

The Cas9/sgRNA constructs were transformed into *Agrobacterium* strain EHA105 by electroporation. *Agrobacterium tumefaciens*-mediated transformation of tomato (*Solanum lycopersicum*) cultivar *Ailsa Craig* were performed according to McCormick (1991). Plantlets were acclimated to become sturdy plants before transfer to the harsher conditions of the glasshouse. All tomato lines were grown in the UK under standard glasshouse conditions of 16-h day length and 25°C, with a night temperature of 18°C. Supplemental lighting was provided where required. Plants from each genotype were grown in "CNSC" coarse potting compost (Levington) in 7.5 L pots with irrigation supplemented with Vitax 214 with pot locations randomized throughout the glasshouse.

Transgenic Verification, Genotyping, and Segregation of Targeted Mutagenesis in T1 Generation

Leaflets were collected from each T_0 plant and genomic DNA was extracted using ISOLATE II Plant DNA Kit (BIOLINE). The presence of the Cas9/sgRNA transgene was verified by PCR with primers pAGM4723 F3/R3 (Supplemental Table S5) designed to amplify a region spanning a 1,652-bp coding region of Cas9. To detect CRISPR/Cas9-induced mutations, the genomic regions surrounding the target sites were amplified using specific PCR primers (Supplemental Table S5). The fragments were directly sequenced or cloned into the pJET1.2/blunt vector and sequenced. The genotypes were also examined to investigate the transmission pattern of CRISPR/Cas9-mediated mutations. T1 progeny were obtained by strict self-pollination. For each T_0 line, 10 to 20 progeny were randomly selected and examined by sequencing.

qRT-PCR

Total RNA from tomato fruit pericarp at breaker+7 was extracted with Spectrum TM Plant Total RNA Kit (Sigma-Aldrich). Five-hundred nanograms of total RNA was reverse-transcribed into 20 μL cDNA using SuperScript III First-Strand Synthesis SuperMix (Invitrogen) following the manufacturer's instructions. The qPCR amplification was carried out using PerfeCTa SYBR Green SuperMix (Quanta Biosciences). A 10 μL reaction mixture was set up and contained 5 μL PerfeCTa SYBR Green SuperMix (2×), 0.3 μL forward/reverse primer (10 μM), and an input quantity of cDNA corresponding to 0.25 ng of total RNA with ddH_2O. Four experimental replicates were performed for each sample. RT-qPCR was run on a LightCycler480 System (Roche Applied Science); PCR conditions were as follows: an initial denaturation step at 95°C for 10 min, followed by 45 cycles of 95°C for 15 s, and 60°C for 60s, with a final cooling step at 40°C for 10 min. The *ELONGATION FACTOR1-ALPHA* gene was used as an internal control. Gene-specific primers for RT-qPCR are listed in Supplemental Table S6. The relative expression levels were calculated using the relative standard curve method and expressed as the relative quantity of target normalized to the reference gene *ELONGATION FACTOR1-ALPHA*.

Physiochemical Analysis and Mechanical Measurement of Fruit Texture

Fruit CI was recorded using a CR400 colorimeter (Minolta). Readings were taken based on the L^*, a^*, and b^* Hunter color scale and CI value was calculated from the equation $CI = (2000 \times a^*)/ [L^* \times (a^{*2} + b^{*2})^{1/2}]$ (López Camelo and Gómez, 2004). Soluble solids were recorded as % Brix and measured by a hand-held refractometer. The mechanical properties of fruit were measured using probe penetration tests using an LF Plus machine (Lloyd Instruments) equipped with a 10 N load cell and 1.6-mm flat-head cylindrical probe as described by Uluisik et al. (2016). Measurements were taken separately from the outer and inner pericarp in duplicate.

Viscosity Analysis of Tomato Paste

The tomato fruit was peeled and halved. Seeds and locular tissue were removed and the pericarp was ground in a coffee grinder for 30 s to make the puree. Stirred viscosity was measured at 20°C based on a 200-mL volume of puree using a RheoLabQC Quality Control Rheometer (Anton Paar) installed with the Rheoplus software according to the manufacturer's instructions (Device: RheolabQC SN910545; FW1.24; Application: RHEOPLUS/32 Multi3 V3.40 21004817-33028; Measure system: CC27/S-SN18049; $d = 0$ mm). For each sample, viscosity was measured against a range of shear rates changing from 1 to 100 [1/s] on a logarithmic setting at 11 measurement points so that the measuring profile had shear rate $d(\gamma)/dt = 1 \ldots 100$ 1/s log; |Slope| = 5 measurement points/decade.

Determination of PG Activity, β-Galactosidase Activity, and β-Galactanase Activity

Enzyme extracts were made from 5 g of frozen pericarp sampled at breaker +7 stage following the methods described by Pressey (1983). Frozen tomato pericarp tissue was ground with a coffee grinder into fine powder. All subsequent steps were conducted at 4°C. This powder was then homogenized with 20 mL ddH_2O and the suspension was stirred for 30 min. Solid NaCl was added to a final concentration of 1.0 M and pH was adjusted to 6.0 with 1.0 M NaOH. The suspension was then stirred for an additional 1 h. The supernatant was collected after centrifugation at 8000*g* for 20 min and ammonium sulfate was added to 80% of saturation. Protein was allowed to precipitate overnight and collected by centrifugation at 16,000*g* for 30 min. The pellet was resuspended with 2 mL 80% ammonium sulfate. Protein concentrations of crude enzyme

solutions were measured by the Bradford method (Bradford, 1976) using a Quick Start Bradford Protein Assay Kit (Bio-Rad).

Determination of PG activity was based on the analysis of reducing groups released from polygalacturonic acid substrate (Honda et al., 1982). Beta-Galactosidase activity was assayed by measuring the rate at which the enzyme hydrolyzed p-nitrophenyl-p-D-galactopyranoside (Pressey, 1983). TBG4 (Exo-galactanase) was assayed by measuring the release of monomeric D-(+)-Gal against a potato RG-I pretreated with arabinofuranosidase (Megazyme) following methods described in Carey et al. (1995).

Determination of PL Enzyme Activity

PL activity was estimated by the method described in Uluisik et al. (2016) and based on Collmer et al. (1988). For preparation of the acetone insoluble solids (AIS), 20 g of fresh pericarp (breaker+7) was homogenized with cold 80% (v/v) acetone. The sample was washed with 100% acetone to remove all pigment and the powder left overnight to dry at room temperature. Then 5 mg of the AIS was stirred for 30 min in 1.9 mL of 8.5M Tris-HCL at 20°C. The samples were then centrifuged for 30 min at 14,000 rpm, and the absorbance of clear supernatant was measured at 232 nm, for determination of the level of reaction products with double bonds released as a result of PL activity. Controls were conducted using a parallel assay where the AIS was inactivated by boiling in 80% (v/v) ethanol.

Carotenoid Analysis

Carotenoids were extracted from 10 mg of freeze-dried fruit as described in Fraser et al. (2000) by the addition of chloroform:methanol:water (2:1:1). Phase separation was facilitated by centrifugation of the mixture and the organic phase containing carotenoids was collected and taken to dryness under vacuum centrifugation (Genevac EZ.27). Dried samples were stored at −20°C and redissolved in ethyl acetate before chromatographic analysis.

Carotenoids were separated and identified by ultra-HPLC with photo diode array detection as described in Uluisik et al. (2016). An Acquity UPLC (Waters) was used with a BEH C18 column (2.1 × 100 mm, 1.7 μm) with a BEH C18 VanGuard precolumn (2.1 × 50 mm, 1.7 μm). The mobile phase used was A: MeOH/H2O (50/50) and B: ACN (acetonitrile)/ethyl acetate (75:25) at a flow rate of 0.5 mL/min. All solvents used were HPLC grade and filtered before use through a 0.2-μm filter. The gradient was 30%:70% (A:B) for 0.5 min, stepped to 0.1%:99.9% (A:B) for 5.5 min, and then stepped to 30%:70% (A:B) for the last 2 min. Column temperature was maintained at 30°C and the samples' temperature at 8°C. On-line scanning across the UV/Vis range was performed in a continuous manner from 250 nm to 600 nm, using an extended wavelength photodiode array (Waters). Carotenoids were quantified from dose-response curves of authentic standards.

Immunofluorescence and Immunocytochemistry Procedures

For immunofluorescence microscopy, tomato fruit were harvested at breaker +4 from a range of CRISPR lines and azygous controls. Two millimeter cubes of pericarp tissue cut from the equatorial sections were fixed in 0.1 M sodium cacodylate buffer and 2% paraformaldehyde (w/v), pH 6.9, overnight at 4°C. Samples were dehydrated by incubation in an ascending ethanol series (30%, 50%, 70%, 90%, and 100% v/v) with 1 h incubation at 4°C for each change. Dehydrated cubes were then infiltrated with resin at 4°C by increasing from 25% resin in ethanol for 2 h, to 50% overnight and then 75% for 8 h and 100% resin overnight. This was followed by a further four changes of absolute ethanol/LR White resin mix. Samples were then placed in 8 mm flat-bottomed TAAB embedding capsules (C094; TAAB Laboratories Equipment) containing LR White Resin and allowed to polymerize at 60°C for 9 h. Then blocks were trimmed and 0.5-μm sections were cut using a Diatome Ultra 45° diamond knife on an EM UC7 ultramicrotome (Leica) and collected onto 6.7-mm 10-well cavity diagnostic slides (Thermo Fisher Scientific) precoated with 2% (3-aminopropl) triethoxysilane in acetone.

For the in situ labeling procedures, rat monoclonal antibodies LM19 to unesterified HG (Verhertbruggen et al., 2009) and LM5 to 1,4-galactan (Jones et al., 1997; Andersen et al., 2016) were used. Nonspecific binding was blocked with 3% (w/v) solution of fat-free milk powder in PBS (PBS/MP) for at least 30 min and sections were washed with PBS for 5 min. Specimens were incubated with a 10-fold dilution of primary monoclonal antibody diluted in PBS/MP for 2 h at room temperature. They were then washed with three changes of PBS with at least 5 min for each change. After the incubation, they were incubated with a secondary antirat IgG (whole molecule)-FITC antibody (F1763; Sigma-Aldrich) diluted 100-fold in PBS/MP for 1.5 h at room temperature and washed with three changes of PBS with at least 5 min for each change. Samples were mounted using a small drop of Citifluor AF1 glycerol/PBS-based antifade mountant solution (Agar Scientific). Coverslips (22 × 50 mm, NO 1.5) were sealed with nail polish. The specimens were examined with a TCS SP5 Confocal Laser Scanning Microscope (Leica) according to the user guide, and micrographs were analyzed with the software ImageJ (Schindelin et al., 2012).

For quantitative assessments of pectic epitopes in sequentially solubilized cell wall fractions, rat monoclonal antibody LM6 to arabinan (Willats et al., 1998) and mouse monoclonal antibody INRA-RU1 to the backbone of RG-I (Ralet et al., 2010) were used in addition to LM19 and LM5. Cell wall material where endogenous pectin-degrading enzymes were inactivated, was prepared as follows: Tomato pericarp was frozen in liquid N_2 and broken into small pieces with a pestle and mortar. The cubes were then boiled in 95% ethanol (100 mL) at 80°C for 30 min. The sample was cooled to room temperature, homogenized using a Polytron Homogenizer and then filtered through Miracloth and washed successively with hot 85% ethanol (200 mL), chloroform/methanol (1:1 v/v; 200 mL), and 100% acetone. The samples were then air-dried overnight. This crude cell wall preparation was then used in the fractionation studies. The cell wall materials were sequentially extracted (10 mg in 1 mL) with water, CDTA, 4 M KOH, and with a cellulase treatment of the final insoluble residue to release polysaccharides associated with cellulose microfibrils as described in Posé et al. (2018). Solubilized extracts at dilutions ranging from 250-fold to 31,250-fold were used to coat microtiter plates before ELISA procedures as described in Willats et al. (1998) and Posé et al. (2018).

Transmission Electron Microscopy

Seventy-nanometer–thick sections were cut from resin blocks previously prepared for immunohistochemistry using a Diatome Ultra 45° diamond knife on an EM UC7 ultramicrotome (Leica), and collected onto 3.05-mm copper-mesh grids (Agar Scientific). Grids were contrasted for 30 min in 2% uranyl acetate and washed in pure water, followed by 5 min in Reynolds lead citrate, washed in pure water and allowed to dry. Samples were imaged in a JEM-1400 transmission electron microscope (JEOL) with an accelerating voltage of 100 kV. Images were captured using a Megaview III digital camera with iTEM software.

Statistical Analysis

There were replicate plants from each genetic line. Biological replicates are individual fruit from different plants of the same line. For each parameter, the variation among plants was partitioned by analysis of variance into the variation between and within genetic lines, and the residual variation among plants of the same genetic line was used as the pooled variance estimate for subsequent posthoc pairwise comparisons between means. Dunnet's test was applied when the objective was to compare each mutant line mean to the mean of the wild-type control, and Duncan's multiple range test was used when all possible pairs of means were to be compared.

Accession Numbers

Sequence data from this article can be found in the GenBank/EMBL data libraries under accession numbers *PL* (Solyc03g111690), *PG2a* (Solyc10g080210), *TBG4* (Solyc12g008840), and other *PL* (Solyc05g055510, Solyc02g093580, Solyc06g083580) and *PG* (Solyc08g060970) family members.

Supplemental Data

The following supplemental materials are available.

Supplemental Figure S1. Amino acid sequence analysis of PL in wild-type and CRISPR lines.

Supplemental Figure S2. Amino acid sequence analysis of *PG2a* in wild-type and CRISPR lines.

Supplemental Figure S3. Amino acid sequence analysis of *TBG4* in wild-type and CRISPR lines.

Supplemental Figure S4. Relative expression of target genes in CRISPR mutants in *PL*, *PG2a*, and *TBG4* lines.

Supplemental Figure S5. Expression of *PL* and *PG2a* gene family members in the CRISPR lines at the breaker+7 stage.

Supplemental Figure S6. β-galactosidase activity in *TBG4* CRISPR lines measured as specific activity/mg of protein.

Supplemental Figure S7. Carotenoid levels in the ripe fruits of the CRISPR lines. Carotenoids were extracted at breaker+7 with three biological replicates for each line.

Supplemental Figure S8. Calcofluor white staining of pericarp sections from CRISPR lines.

Supplemental Table S1. Target sequences of cell wall structure-related genes.

Supplemental Table S2. Fresh weight:dry weight of pericarp sections from three independent wild-type and *PG2a*, *PL*, and *TBG4* lines.

Supplemental Table S3. Fluorescence intensity based on analysis of sections in the confocal microscope at 10× objective with the software ImageJ and using Duncan's multiple range test to compare lines.

Supplemental Table S4. Primer sequences for amplifying sgRNAs.

Supplemental Table S5. Primers for genotyping of CRISPR/Cas9-induced mutations.

Supplemental Table S6. Primer sequences for RT-qPCR.

ACKNOWLEDGMENTS

The mouse RG-I antibody INRA-RU1 was kindly provided (to J.P.K.) by Dr. Marie-Christine Ralet and Dr. Fabienne Guillon. We thank Dr. Darren Wells for his help with the confocal microscopy. This work was supported by the Biotechnology and Biological Sciences Research Council [grant number BB/M025918/1]. Graham Seymour would like to thank the Biotechnology and Biological Sciences Research Council and Innovate UK for financial support.

Received September 28, 2018; accepted November 13, 2018; published November 20, 2018.

LITERATURE CITED

Airianah OB, Vreeburg RAM, Fry SC (2016) Pectic polysaccharides are attacked by hydroxyl radicals in ripening fruit: Evidence from a fluorescent fingerprinting method. Ann Bot **117:** 441–455

Andersen MCF, Boos I, Marcus SE, Kračun SK, Rydahl MG, Willats WGT, Knox JP, Clausen MH (2016) Characterization of the LM5 pectic galactan epitope with synthetic analogues of β-1,4-D-galactotetraose. Carbohydr Res **436:** 36–40

Atmodjo MA, Hao Z, Mohnen D (2013) Evolving views of pectin biosynthesis. Annu Rev Plant Biol **64:** 747–779

Bidhendi AJ, Geitmann A (2016) Relating the mechanics of the primary plant cell wall to morphogenesis. J Exp Bot **67:** 449–461

Bradford MM (1976) A rapid and sensitive method for the quantitation of microgram quantities of protein utilizing the principle of protein-dye binding. Anal Biochem **72:** 248–254

Brooks C, Nekrasov V, Lippman ZB, Van Eck J (2014) Efficient gene editing in tomato in the first generation using the clustered regularly interspaced short palindromic repeats/CRISPR-associated9 system. Plant Physiol **166:** 1292–1297

Brummell DA (2006) Cell wall disassembly in ripening fruit. Funct Plant Biol **33:** 103–119

Brummell DA, Harpster MH, Civello PM, Palys JM, Bennett AB, Dunsmuir P (1999) Modification of expansin protein abundance in tomato fruit alters softening and cell wall polymer metabolism during ripening. Plant Cell **11:** 2203–2216

Cantu D, Vicente AR, Greve LC, Dewey FM, Bennett AB, Labavitch JM, Powell ALT (2008) The intersection between cell wall disassembly, ripening, and fruit susceptibility to *Botrytis cinerea*. Proc Natl Acad Sci USA **105:** 859–864

Carey AT, Holt K, Picard S, Wilde R, Tucker GA, Bird CR, Schuch W, Seymour GB (1995) Tomato exo-(1→4)-beta-D-galactanase. Isolation, changes during ripening in normal and mutant tomato fruit, and characterization of a related cDNA clone. Plant Physiol **108:** 1099–1107

Carpita NC, Gibeaut DM (1993) Structural models of primary cell walls in flowering plants: consistency of molecular structure with the physical properties of the walls during growth. Plant J **3:** 1–30

Collmer A, Ried JL, Mount MS (1988) Assay methods for pectic enzymes. Methods Enzymol **161:** 329–335

Cornuault V, Posé S, Knox JP (2018) Disentangling pectic homogalacturonan and rhamnogalacturonan-I polysaccharides: Evidence for sub-populations in fruit parenchyma systems. Food Chem **246:** 275–285

Dellapenna D, Kates DS, Bennett AB (1987) Polygalacturonase gene expression in Rutgers, *rin*, *nor*, and *Nr* tomato fruits. Plant Physiol **85:** 502–507

Dick-Pérez M, Zhang Y, Hayes J, Salazar A, Zabotina OA, Hong M (2011) Structure and interactions of plant cell-wall polysaccharides by two- and three-dimensional magic-angle-spinning solid-state NMR. Biochemistry **50:** 989–1000

Errington N, Tucker GA, Mitchell JR (1998) Effect of genetic down-regulation of polygalacturonase and pectin esterase activity on rheology and composition of tomato juice. J Sci Food Agric **76:** 515–519

Fraser PD, Pinto ME, Holloway DE, Bramley PM (2000) Technical advance: Application of high-performance liquid chromatography with photodiode array detection to the metabolic profiling of plant isoprenoids. Plant J **24:** 551–558

Gao X, Chen J, Dai X, Zhang D, Zhao Y (2016) An effective strategy for reliably isolating heritable and Cas9-free Arabidopsis mutants generated by CRISPR/Cas9-mediated genome editing. Plant Physiol **171:** 1794–1800

Gross KC (1985) Promotion of ethylene evolution and ripening of tomato fruit by galactose. Plant Physiol **79:** 306–307

Honda S, Nishimura Y, Takahashi M, Chiba H, Kakehi K (1982) A manual method for the spectrophotometric determination of reducing carbohydrates with 2-cyanoacetamide. Anal Biochem **119:** 194–199

Ito Y, Nishizawa-Yokoi A, Endo M, Mikami M, Toki S (2015) CRISPR/Cas9-mediated mutagenesis of the *RIN* locus that regulates tomato fruit ripening. Biochem Biophys Res Commun **467:** 76–82

Jiménez-Bermúdez S, Redondo-Nevado J, Muñoz-Blanco J, Caballero JL, López-Aranda JM, Valpuesta V, Pliego-Alfaro F, Quesada MA, Mercado JA (2002) Manipulation of strawberry fruit softening by antisense expression of a pectate lyase gene. Plant Physiol **128:** 751–759

Jones L, Seymour GB, Knox JP (1997) Localization of pectic galactan in tomato cell walls using a monoclonal antibody specific to (1−4)-β-D-galactan. Plant Physiol **113:** 1405–1412

Keegstra K (2010) Plant cell walls. Plant Physiol **154:** 483–486

Kitagawa M, Itoa H, Shiinab T, Nakamurab N, Inakumaa T, Kasumib T, Ishiguroa Y, Yabeb K, Ito Y (2005) Characterization of tomato fruit ripening and analysis of gene expression in F_1 hybrids of the *ripening inhibitor* (*rin*) mutant. Physiol Plant **123:** 331–338

Klee HJ, Giovannoni JJ (2011) Genetics and control of tomato fruit ripening and quality attributes. Annu Rev Genet **45:** 41–59

Lin D, Lopez-Sanchez P, Gidley MJ (2016) Interactions of pectins with cellulose during its synthesis in the absence of calcium. Food Hydrocoll **52:** 57–68

López Camelo A, Gómez PA (2004) Comparison of color indexes for tomato ripening. Hortic Bras **22:** 534–537

Lykke-Andersen S, Jensen TH (2015) Nonsense-mediated mRNA decay: An intricate machinery that shapes transcriptomes. Nat Rev Mol Cell Biol **16:** 665–677

McCartney L, Ormerod AP, Gidley MJ, Knox JP (2000) Temporal and spatial regulation of pectic (1−4)-β-D-galactan in cell walls of developing pea cotyledons: Implications for mechanical properties. Plant J **22:** 105–113

McCormick S (1991) Transformation of tomato with *Agrobacterium tumefaciens*. Plant Tissue Culture Manual. **B6:** 311–319

Melotto E, Greve LC, Labavitch JM (1994) Cell wall metabolism in ripening fruit (VII. Biologically active pectin oligomers in ripening tomato (*Lycopersicon esculentum* Mill.) fruits). Plant Physiol **106:** 575–581

Nekrasov V, Staskawicz B, Weigel D, Jones JDG, Kamoun S (2013) Targeted mutagenesis in the model plant *Nicotiana benthamiana* using Cas9 RNA-guided endonuclease. Nat Biotechnol **31:** 691–693

Pan C, Ye L, Qin L, Liu X, He Y, Wang J, Chen L, Lu G (2016) CRISPR/Cas9-mediated efficient and heritable targeted mutagenesis in tomato plants in the first and later generations. Sci Rep **6:** 24765

Paniagua C, Blanco-Portales R, Barceló-Muñoz M, García-Gago JA, Waldron KW, Quesada MA, Muñoz-Blanco J, Mercado JA (2016) Antisense down-regulation of the strawberry β-galactosidase gene *FaβGal4* increases cell wall galactose levels and reduces fruit softening. J Exp Bot **67:** 619–631

Pecker I, Gabbay R, Cunningham FX, Jr., Hirschberg J (1996) Cloning and characterization of the cDNA for lycopene β-cyclase from tomato reveals decrease in its expression during fruit ripening. Plant Mol Biol **30:** 807–819

Popper ZA, Fry SC (2005) Widespread occurrence of a covalent linkage between xyloglucan and acidic polysaccharides in suspension-cultured angiosperm cells. Ann Bot **96:** 91–99

Popper ZA, Fry SC (2008) Xyloglucan-pectin linkages are formed intraprotoplasmically, contribute to wall-assembly, and remain stable in the cell wall. Planta **227:** 781–794

Posé S, Kirby AR, Paniagua C, Waldron KW, Morris VJ, Quesada MA, Mercado JA (2015) The nanostructural characterization of strawberry pectins in pectate lyase or polygalacturonase silenced fruits elucidates their role in softening. Carbohydr Polym **132:** 134–145

Posé S, Marcus SE, Knox JP (2018) Differential metabolism of pectic galactan in tomato and strawberry fruit: Detection of the LM26 branched galactan epitope in ripe strawberry fruit. Physiol Plant **164:** 95–105

Pressey R (1983) beta-Galactosidases in ripening tomatoes. Plant Physiol **71:** 132–135

Quesada MA, Blanco-Portales R, Posé S, García-Gago JA, Jiménez-Bermúdez S, Muñoz-Serrano A, Caballero JL, Pliego-Alfaro F, Mercado JA, Muñoz-Blanco J (2009) Antisense down-regulation of the *FaPG1* gene reveals an unexpected central role for polygalacturonase in strawberry fruit softening. Plant Physiol **150:** 1022–1032

Ralet MC, Tranquet O, Poulain D, Moïse A, Guillon F (2010) Monoclonal antibodies to rhamnogalacturonan I backbone. Planta **231:** 1373–1383

Redgwell RJ, MacRae E, Hallett I, Fischer M, Perry J, Harker R (1997) *In vivo* and *in vitro* swelling of cell walls during fruit ripening. Planta **203:** 162–173

Round AN, Rigby NM, MacDougall AJ, Morris VJ (2010) A new view of pectin structure revealed by acid hydrolysis and atomic force microscopy. Carbohydr Res **345:** 487–497

Saladié M, Matas AJ, Isaacson T, Jenks MA, Goodwin SM, Niklas KJ, Xiaolin R, Labavitch JM, Shackel KA, Fernie AR, et al (2007) A reevaluation of the key factors that influence tomato fruit softening and integrity. Plant Physiol **144:** 1012–1028

Schindelin J, Arganda-Carreras I, Frise E, Kaynig V, Longair M, Pietzsch T, Preibisch S, Rueden C, Saalfeld S, Schmid B, et al (2012) Fiji: An open-source platform for biological-image analysis. Nat Methods **9:** 676–682

Schuch W, Kanczler J, Robertson D, Hobson G, Tucker G, Grierson D, Bright S, Bird C (1991) Fruit quality characteristics of transgenic tomato fruit with altered polygalacturonase activity. HortScience **26:** 1517–1520

Sesmero R, Mitchell JR, Mercado JA, Quesada MA (2009) Rheological characterisation of juices obtained from transgenic pectate lyase-silenced strawberry fruits. Food Chem **116:** 426–432

Seymour GB, Colquhoun IJ, Dupont MS, Parsley KR, Selvendran RR (1990) Composition and structural features of cell-wall polysaccharides from tomato fruits. Phytochemistry **29:** 725–731

Seymour GB, Østergaard L, Chapman NH, Knapp S, Martin C (2013) Fruit development and ripening. Annu Rev Plant Biol **64:** 219–241

Shan Q, Wang Y, Li J, Gao C (2014) Genome editing in rice and wheat using the CRISPR/Cas system. Nat Protoc **9:** 2395–2410

Sheehy RE, Kramer M, Hiatt WR (1988) Reduction of polygalacturonase activity in tomato fruit by antisense RNA. Proc Natl Acad Sci USA **85:** 8805–8809

Shimatani Z, Kashojiya S, Takayama M, Terada R, Arazoe T, Ishii H, Teramura H, Yamamoto T, Komatsu H, Miura K, et al (2017) Targeted base editing in rice and tomato using a CRISPR-Cas9 cytidine deaminase fusion. Nat Biotechnol **35:** 441–443

Smith DL, Gross KC (2000) A family of at least seven β-galactosidase genes is expressed during tomato fruit development. Plant Physiol **123:** 1173–1183

Smith CJS, Watson CF, Ray J, Bird CR, Morris PC, Schuch W, Grierson D (1988) Antisense RNA inhibition of polygalacturonase gene-expression in transgenic tomatoes. Nature **334:** 724–726

Smith CJ, Watson CF, Morris PC, Bird CR, Seymour GB, Gray JE, Arnold C, Tucker GA, Schuch W, Harding S, et al (1990) Inheritance and effect on ripening of antisense polygalacturonase genes in transgenic tomatoes. Plant Mol Biol **14:** 369–379

Smith DL, Abbott JA, Gross KC (2002) Down-regulation of tomato beta-galactosidase 4 results in decreased fruit softening. Plant Physiol **129:** 1755–1762

Sun Y, Zhang X, Wu C, He Y, Ma Y, Hou H, Guo X, Du W, Zhao Y, Xia L (2016) Engineering herbicide-resistant rice plants through CRISPR/Cas9-mediated homologous recombination of acetolactate synthase. Mol Plant **9:** 628–631

Svitashev S, Schwartz C, Lenderts B, Young JK, Mark Cigan A (2016) Genome editing in maize directed by CRISPR-Cas9 ribonucleoprotein complexes. Nat Commun **7:** 13274

Thankur B, Singh R, Nelson P (1996) Quality attributes of processed tomato products: A review. Food Rev Int **12:** 375–401

Thomas LH, Forsyth VT, Sturcová A, Kennedy CJ, May RP, Altaner CM, Apperley DC, Wess TJ, Jarvis MC (2013) Structure of cellulose microfibrils in primary cell walls from collenchyma. Plant Physiol **161:** 465–476

Thompson JE, Fry SC (2000) Evidence for covalent linkage between xyloglucan and acidic pectins in suspension-cultured rose cells. Planta **211:** 275–286

Tieman DM, Handa AK (1994) Reduction in pectin methylesterase activity modifies tissue integrity and cation levels in ripening tomato (*Lycopersicon esculentum* Mill.) fruits. Plant Physiol **106:** 429–436

Tomato Genome Consortium (2012) The tomato genome sequence provides insights into fleshy fruit evolution. Nature **485:** 635–641

Uluisik S, Chapman NH, Smith R, Poole M, Adams G, Gillis RB, Besong TMD, Sheldon J, Stiegelmeyer S, Perez L, et al (2016) Genetic improvement of tomato by targeted control of fruit softening. Nat Biotechnol **34:** 950–952

Verhertbruggen Y, Marcus SE, Haeger A, Ordaz-Ortiz JJ, Knox JP (2009) An extended set of monoclonal antibodies to pectic homogalacturonan. Carbohydr Res **344:** 1858–1862

Wang T, Hong M (2016) Solid-state NMR investigations of cellulose structure and interactions with matrix polysaccharides in plant primary cell walls. J Exp Bot **67:** 503–514

Wang D, Yeats TH, Uluisik S, Rose JKC, Seymour GB (2018) Fruit softening: Revisiting the role of pectin. Trends Plant Sci **23:** 302–310

Wang T, Zabotina O, Hong M (2012) Pectin-cellulose interactions in the Arabidopsis primary cell wall from two-dimensional magic-angle-spinning solid-state nuclear magnetic resonance. Biochemistry **51:** 9846–9856

Wang T, Park YB, Cosgrove DJ, Hong M (2015) Cellulose-pectin spatial contacts are inherent to never-dried arabidopsis primary cell walls: Evidence from solid-state nuclear magnetic resonance. Plant Physiol **168:** 871–884

Wang Y, Cheng X, Shan Q, Zhang Y, Liu J, Gao C, Qiu J-L (2014) Simultaneous editing of three homoeoalleles in hexaploid bread wheat confers heritable resistance to powdery mildew. Nat Biotechnol **32:** 947–951

Weber E, Gruetzner R, Werner S, Engler C, Marillonnet S (2011) Assembly of designer TAL effectors by Golden Gate cloning. PLoS One **6:** e19722

Willats WGT, Marcus SE, Knox JP (1998) Generation of monoclonal antibody specific to (1→5)-alpha-L-arabinan. Carbohydr Res **308:** 149–152

Willats WG, Orfila C, Limberg G, Buchholt HC, van Alebeek GJ, Voragen AG, Marcus SE, Christensen TM, Mikkelsen JD, Murray BS, et al (2001) Modulation of the degree and pattern of methyl-esterification of pectic homogalacturonan in plant cell walls. Implications for pectin methyl esterase action, matrix properties, and cell adhesion. J Biol Chem **276:** 19404–19413

Xu R-F, Li H, Qin R-Y, Li J, Qiu C-H, Yang Y-C, Ma H, Li L, Wei P-C, Yang J-B (2015) Generation of inheritable and "transgene clean" targeted genome-modified rice in later generations using the CRISPR/Cas9 system. Sci Rep **5:** 11491

Yang L, Huang W, Xiong F, Xian Z, Su D, Ren M, Li Z (2017) Silencing of SlPL, which encodes a pectate lyase in tomato, confers enhanced fruit firmness, prolonged shelf-life and reduced susceptibility to grey mould. Plant Biotechnol J **15:** 1544–1555

Yeats TH, Rose JKC (2013) The formation and function of plant cuticles. Plant Physiol **163:** 5–20